Accepted Manuscript

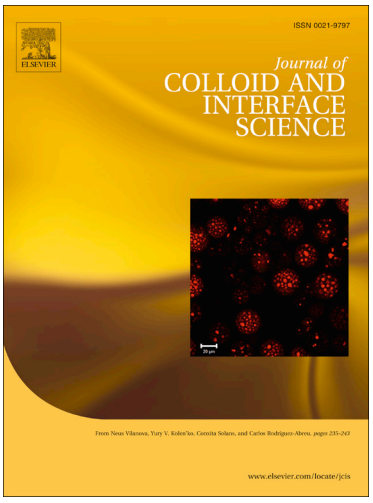

Novel low-fouling membranes from lab to pilot application in textile wastewater treatment

Francesco Galiano, Ines Friha, Shamim Ahmed Deowan, Jan Hoinki, Ye Xiaoyun, Daniel Johnson, Raffaella Mancuso, Nidal Hilal, Bartolo Gabriele, Sami Sayadi, Alberto Figoli

PII: S0021-9797(18)30009-2
DOI: https://doi.org/10.1016/j.jcis.2018.01.009
Reference: YJCIS 23167

To appear in: *Journal of Colloid and Interface Science*

Received Date: 27 November 2017
Revised Date: 22 December 2017
Accepted Date: 3 January 2018

Please cite this article as: F. Galiano, I. Friha, S. Ahmed Deowan, J. Hoinki, Y. Xiaoyun, D. Johnson, R. Mancuso, N. Hilal, B. Gabriele, S. Sayadi, A. Figoli, Novel low-fouling membranes from lab to pilot application in textile wastewater treatment, *Journal of Colloid and Interface Science* (2018), doi: https://doi.org/10.1016/j.jcis.2018.01.009

Novel low-fouling membranes from lab to pilot application in textile wastewater treatment

Francesco Galiano[a], *Ines Friha*[b], *Shamim Ahmed Deowan*[c], *Jan Hoinki*[d,*], *Ye Xiaoyun*[d], *Daniel Johnson*[e,f], *Raffaella Mancuso*[g], *Nidal Hilal*[e,f], *Bartolo Gabriele*[g], *Sami Sayadi*[b], *Alberto Figoli*[a,*]

[a]Institute on Membrane Technology, ITM-CNR, Via P. Bucci, Cubo 17/C, I-87030 Rende, Italy; a.figoli@itm.cnr.it

[b]Center of Biotechnologie of Sfax, Route Sidi Mansour Km6, P.O.Box 1177, 3018 Sfax, Tunisia

[c]Department of Robotics and Mechatronics Engineering, University of Dhaka, Bangladesh

[d]Institute of Applied Research (IAF), Karlsruhe University of Applied Sciences, Moltkestr. 30, 76133 Karlsruhe, Germany; jan.hoinkis@hs-karlsruhe.de

[e]Center for Water Advanced Technologies and Environmental Research (CWATER), College of Engineering, Swansea University, Swansea SA28PP, United Kingdom

[f]Qatar Environment and Energy Research Institute (QEERI), Doha, Qatar

[g]Department of Chemistry and Chemical Technologies, University of Calabria, Via P. Bucci cubo 12/C, 87036 Arcavacata di Rende (CS), Italy

Keywords:

Polymerisable bicontinuous microemulsion (PBM); low fouling membranes; wastewater treatment; membrane bioreactor (MBR); lab to pilot (LTP); textile wastewater

Abstract

A novel antifouling coating based on the polymerization of a polymerisable bicontinuous microemulsion (PBM) was developed and applied for commercially available membranes for textile wastewater treatment. PBM coating was produced by polymerizing, on a polyethersulfone (PES) membrane, a bicontinuous microemulsion, realized by finely tuning its properties in terms of chemical composition and polymerization temperature. In particular, the PBM was prepared by using, as the surfactant component, inexpensive and commercially available dodecyltrimethylammonium bromide (DTAB). The coating exhibited a more hydrophilic and a smoother surface in comparison to uncoated PES surface, making the produced PBM membranes more resistant and less prone to be affected by fouling. The anti-fouling potential of PBM membranes was assessed by using humic acid (HA) as a model foulant, evaluating the water permeability decrease as an indicator of the fouling propensity of the membranes. PBM membrane performances in terms of dye rejection, when applied for model textile wastewater treatment, were also evaluated and compared to PES commercial ones. The PBM membranes were finally successfully scaled-up (total membrane area 0.33 m^2) and applied in a pilot membrane bioreactor (MBR) unit for the treatment of real textile wastewater.

1. Introduction

Due to growing demand and limited availability of fresh water, alternative sources of water are becoming increasingly important day by day. In this context, reuse of treated wastewater offers a viable option to reduce freshwater consumption and, in this regard, membrane bioreactor (MBR) technology plays an important role. Since the regulation of wastewater has noticeably increased in many countries, MBR can be an attractive option for wastewater treatment [1]. The textile industry is considered as one of the most water consuming sectors due to its high demand of water for all parts of its processes. The wastewater discharged by the textile industry contains large amounts of dissolved organic matter, inorganic substances,

has a high pH value and a low BOD/COD ratio [2], dyestuffs and additives, which make it a difficult industrial wastewater to treat. The main environmental concern is related to the large amount of dyes (used in the dyeing process) which are poorly biodegradable and not efficiently removed by conventional activated sludge plants [3]. Moreover, their presence in water effluents can have negative effects on the photosynthetic process of aquatic life [4]. Biodegradability of dyes as well as the removal of colour is a major issue, which has been discussed in the literature [5-7]. Moreover, the removal of dyes from textile wastewater, due to its persistent nature and the types of dyes, is not an easy task. To deal with the problems associated with textile effluents, several studies have been directed at the treatment of polluted streams close to the point of source, as in the integrated approach [8-10] and at the treatment of the final effluents (end of pipe approach) [11-14]. MBR technology, which combines the benefits of high biomass concentrations with the possibility to run a continuous process at controlled biomass retention [2], is recognised as a promising technology to provide water with reliable quality for re-use, and it is very attractive for industrial wastewater treatment [15-17]. Since the membrane costs have decreased dramatically over the last years to currently approximately 50 Euro/m^2 [18] and energy requirements for aeration of the membrane are also fast approaching the normal activated sludge process (ASP) range, this has now become an economically feasible solution for wastewater treatment. Due to low biodegradability of textile dyes under aerobic conditions in conventional ASP, a large reactor volume is necessary, while MBR reduces the required reactor volume [2]. Today MBRs are robust, simple to operate and even more affordable. They take up reduced footprint, need modest technical support and can remove many contaminants in one step. This makes them practical to safely reuse water for non-potable uses.

However, fouling of membranes used in MBR applications by textile wastewater is still a big obstacle. Once the membrane is faced with fouling and the extensive chemical cleaning cannot restore the flux [19], the membrane needs to be replaced which may account for up to

30-50% of the operation cost. In MBRs, fouling can be attributed to pore blocking (deposition within the pores) or to cake layer formation on the membrane surface [20]. Colloidal and soluble foulants (SMP) can cause pore blocking and irreversible fouling due to their small size. To mitigate fouling problems, many researchers have followed different techniques [15]. In addition to those techniques, influent pre-treatment (physical, chemical, biological), combination of MBR with other technologies, influent pH adjustment, optimization of operation conditions, hydrodynamic control of a filtration system, proper design and operation, application of membrane performance enhancer (MOE) etc. can be applied/adapted to lower the fouling problems. Moreover, several theoretical models were proposed in order to understand the fundamentals of fouling formation in MBRs in order to mitigate this phenomenon [21-23]. Suitable membrane surface modification can represent another promising approach to mitigate the fouling [24-26]. Different approaches have been proposed so far in order to mitigate fouling formation by coating different materials such as other polymers (like polyvinyl alcohol (PVA)) [27]; silica nanoparticles [28], dopamine [29] and graphene-oxide [30].

In this contest, we report here a novel low-fouling membrane material based on the polymerizable bicontinuous microemulsion (PBM) technology, which makes use of an unexpensive and commercially available surfactant dodecyltrimethylammonium bromide (DTAB) in PBM preparation.

Microemulsions were characterized in terms of ternary phase diagram and conductivity measurements to identify the proper chemical composition. Further characterizations (SEM, AFM and CAM) were aimed to the investigation of membrane surface properties and morphology. Preliminary tests with HA were carried out in order to assess the anti-fouling potential of PBM membranes. The performances of PBM membranes were also evaluated in terms of dye rejection in model textile wastewater.

The membranes produced were successfully applied for the first time in a pilot scale operation for the treatment of real raw textile wastewater (RTW).

2. Materials and methods

2.1 Microemulsion composition

The novel PBM low fouling membrane, used for the MBR treatment, was obtained by following the polymerization procedure described by Galiano et al. [25]. The chemicals used for preparing PBM membranes were: methyl methacrylate (MMA) used as monomer constituting the oil phase of the microemulsion, 2-hydroxyethyl methacrylate (HEMA) used as co-surfactant and the commercial dodecyltrimethylammonium bromide (DTAB) used as a surfactant for stabilizing the microemulsion. Ethylene glycol dimethacrylate (EGDMA) was used as a cross-linking agent. Ammonium persulfate (APS) and N,N,N´N´-tetramethylethylenediamine (TMEDA) were used as redox initiators in order to promote the polymerization process. All the chemicals used for preparing microemulsions were purchased from Sigma-Aldrich with purity higher than 98% (analytical grade).

2.2 Phase diagram and microemulsion conduxtivity

To investigate the microemulsion regions with the commercial surfactant (DTAB) a phase diagram was constructed by the titration method. Firstly, a mixture of DTAB and HEMA at the weight ratio of 1:4 was prepared. Then, MMA was added to the DTAB/HEMA mixture at the weight ratio of 1:9, 2:8, 3:7, 4:6, 5:5, 6:4, 7:3, 8:2 and 9:1. The boundaries of the microemulsion domains were finally identified by titrating dropwise with water at room temperature and classified as microemulsions when they appeared completely transparent.

Conductivity measurements for the determination of the microemulsion regions were carried out by Eutech Instruments PC 2700. Microemulsions were prepared at different aqueous solutions containing 20 wt% of the surfactant DTAB. EGDMA added was 4 wt% based on the weight of total MMA and HEMA used. MMA:HEMA ratio was maintained 1:4. The measurements were carried out at room temperature (25°C) and each measurement was repeated three times and the average was considered.

2.3 Microemulsion preparation and polymerization

The microemulsion was prepared in a double-necked round bottom volumetric flask. Firstly, the monomer MMA and co-surfactant HEMA were mixed. Next, water was added to the system followed by DTAB. The solution was then mechanically stirred for 5 minutes and when a clear and transparent system was obtained, the cross-linker EGDMA was added. Then, the redox initiator APS and TMEDA were added to a concentration of 0.3 wt% and 20 mM, respectively. The microemulsion was purged with nitrogen gas and left to react. The microemulsion was then cast on a commercial polyethersulfone (PES) ultrafiltration (UF) membrane (NADIR® PM UP 150, Microdyn-Nadir, 2015) in an inert N_2 gas saturated casting chamber.

The casting knife thickness used was 250 µm. A N_2 saturated environment was needed to exclude any contact with air or oxygen since it can interfere with the polymerization process. The temperature of the casting chamber was varied from 20 to 50°C. The membrane sheets with dimensions of 30 cm×30 cm were made and then laminated, in collaboration with Microdyn-Nadir (Germany), for the production of the envelopes to be used as MBR module. The membrane module, including the 3 envelopes produced, possessed an active membrane surface of 0.33 m^2. The novel coated PBM membranes applied for MBR and the non-coated PES membranes applied for MBR were named as PBM MBR and PES MBR modules, respectively. All the polymerized membranes were pre-treated before use (to remove the

glycerol used as a pore filling agent for PES commercial membranes) with an initial aqueous solution containing 25 wt% of isopropanol followed by further washing with distilled water overnight.

2.4 Weight loss determination and contact angle measurements

In order to determine whether all the material used for microemulsion polymerization was polymerised in the coating network, the pure PBM membranes (not coated on PES support) were dried up and exposed to subsequent extractions. First, the polymerised membrane was dried up in order to remove the water, then it was extracted with toluene for 2h in order to remove unpolymerised MMA and HEMA and finally it was extracted with water at 50°C in order to remove the unreacted surfactant. The amount of unreacted material was determined by measuring the weight loss after each extraction. The loss was calculated by using the following equation (Eq. 1):

$$W_l = \frac{W_i - W_f}{w_f} \cdot 100 \qquad (1),$$

Where:

W_l is the weight loss, w_i is the initial weight of the membrane before each drying or extraction and w_f is the final weight of the membrane after each drying or extraction.

The water contact angle of the produced membranes was measured by the sessile drop method using a CAM200 instrument (KSV Instrument LTD, Finland). Water CAM was carried out on the top side of PES commercial and on the coating side of PBM membranes. A water droplet of 5 µL was deposited on the membrane with a microliter syringe. For each membrane sample, five measurements were taken; average values and standard deviations were then calculated.

2.5 Scanning electron microscopy (SEM), atomic force microscopy (AFM) and infrared spectroscopy (FT-IR)

SEM measurements were carried out using a model S-4800 Field Emission SEM (Hitachi, Japan). All samples were coated with a thin (approximately 15 nm) layer of gold by sputter coating prior to measurement.

AFM observations were all carried out using a Multimode AFM with a Nanoscope IIIa electronic control unit (Veeo, USA). Measurements were all undertaken under ambient laboratory conditions using tapping mode. TESP cantilevers (Bruker AXS, nominal spring constant 20-80 N/m) were used for all measurements. Image resolution was set at values of 512x512 pixels.

The presence and the stability of the PBM coating on PES membrane surface was determined by FT-IR ATR Spectrometer (Perkin Elmer, Spectrum One). In case of PBM membrane, the FT-IR was carried out before and after wasing the membrane using the following protocol:

- 1 h washing with an alcoholic solution (25 wt% isopropanol);
- 72 h washing with distilled water.

2.6 Cross-flow set-up

The lab scale experiments were performed using a cross-flow auto-controlled set-up purchased from SIMA-tec GmbH, Germany (Fig. 1). This testing unit was equipped with heat-exchanger/temperature controller (2) and LabVIEW program based computerized data acquisition system. To abate the vibration of the unit, it was equipped with a damping system (9) by filling the vibration controller with N_2 gas at 16 bar pressure. The experiments with this unit were carried out continuously for a longer time period (from some hours to several days).

For fouling tests, humic acid (HA) was applied since many fundamental studies of the fouling phenomena have been done by using the readily analyzed HA as a model foulant [31]. In addition, HA is representative of foulants in the biological sludge system.

The experiment was run for 24h with distilled (DI) water and then, the HA solution was used as test media. The test was run for a further 3 h, replacing the running fluid with fresh DI water after each hour and the water permeability (WP) regain was calculated using the following Eq. (2).

$$WP = \frac{WP_f - WP_i}{WP_i} \; x\,100 \qquad (2),$$

Where,

WP_f = Final water permeability after 3rd cleanings with DI water

WP_i = Initial water permeability after 24h test run with HA

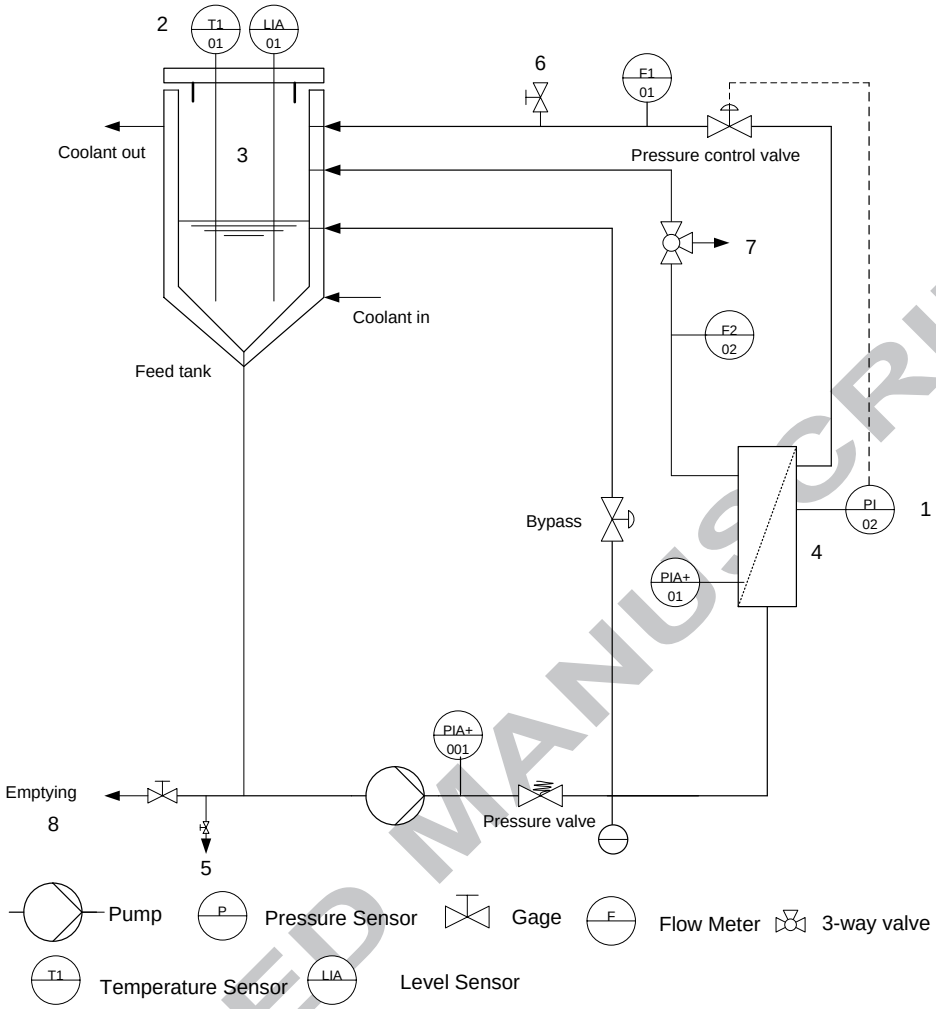

1: Pressure control, 2: Temperature control, 3: Feed tank, 4: Membrane module, 5: Permeate sampling valve, 6: Concentrate sampling valve, 7: Feed sampling valve, 8: drain valve

Fig. 1. Schematic diagram of auto-controlled UF cross-flow cell

2.7 MBR pilot plant

The schematic experimental setup is shown in figure 2. Two aerobic MBRs having working volumes of 60 L each were operated in parallel. The first MBR was coupled to commercial PES membranes (denoted as PES-MBR) while the second one was operated with novel PBM membranes (denoted as PBM-MBR). The operating trans-membrane pressure (TMP) ranged

between 70 and 350 mbar. Both membrane modules were equipped with air diffusers and sludge drains. The reactors were seeded with 60 L of sludge derived from an industrial standard activated sludge plant treating textile wastewaters. The starting mixed liquor suspended solids (MLSS) concentration for both reactors was about 6 g/L and the aeration rate ranged from 1 to 2m^3/h. The MBRs were fed through peristaltic pumps (Minipuls 3 Gilson Model 312, France) synchronized to permeate suction pumps (Watson-Marlow 505U, Falmouth, Cornwall TR11 4RU, England). Two pressure gauges (S-Wika EN 837-1, Germany) were mounted between the membranes and the permeate pumps to monitor the TMP. The reactors were operated at preset flow rates (corresponding to fixed hydraulic retention times HRTs) that were controlled by adjusting the rotation speed of the filtration pumps.

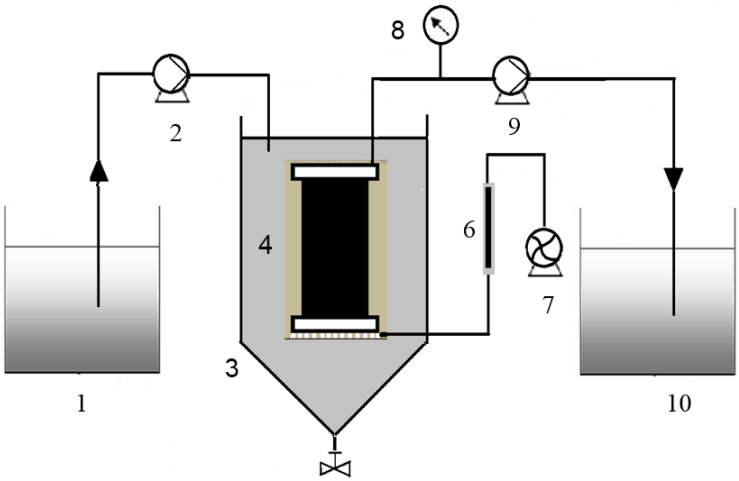

1: Feed tank; 2: Feed pump; 3: MBR reactor; 4: MBR module; 5: Exhaust valve; 6: Compressed air regulator; 7: Compressor; 8: Pressure sensor; 9: Suction pump; 10: Permeate collection tank

Fig. 2. Schematic diagram of the experimental set-up

The flux was measured volumetrically in a measuring cylinder by collecting the permeate over a known period of time. Membrane cleaning, if required, to maintain the imposed permeate flux, was performed by rinsing with tap water.

Wastewater, supernatant of the reactor and treated water were sampled either 3 times a week or on a day interval, stored at 4°C until analysis and were then analyzed for COD and color measurements.

2.8 Textile wastewaters

2.8.1 Model textile dye wastewater (MTDW)

The model textile dye wastewater (MTDW) was based on a red reactive dye (Acid Red 4) denoted as red, and a blue anthraquinone dye (Remazol Brilliant Blue R), denoted as blue in this paper, representing typical industrial dyes widely applied in the textile industry. These chemicals were all bought from Sigma Aldrich, Germany. A typical industrial detergent (Albatex DBC) (from Huntsman Textile Effects GmbH, Germany) and glucose (from Merck GmbH, Germany) were added as a C-source as well as the following salts: NaCl, $NaHCO_3$ and NH_4Cl (N-source) (Merck GmbH, Germany). The tests with the novel PBM coated membrane were carried out in the cross-flow set-up to verify the dye rejections only. The compositions of the applied chemicals are shown in Table 1 below.

Table 1: Composition of the model textile dye wastewater (MTDW) (15)

No.	Dyestuffs and chemicals	Concentration (mg/L)
1	Remazol Brilliant Blue R	50
2	Acid Red 4	50
3	NaCl	2500
4	$NaHCO_3$	1000

5	Glucose	2000
6	Albatex DBC (Detergent)	50
7	NH_4Cl	300

2.8.2 Industrial textile wastewater

The study was conducted with real RTW samples supplied from the Tunisian textile factory SITEX located in Kasr Hellal, Tunisia. The company production line comprises dying fabrics and finishing processes and utilizes different dyes (reactive, direct and sulphur) and chemical substances such as detergents, salts, auxiliaries (e.g. surfactants, emulsifiers). Their amounts depend on the kind of process that generates different effluents. The aerobic consortium used as seed culture for the pilot plant was a sample of the sedimentation sludge from a full-scale activated sludge plant treating textile liquid wastes with some organic nutrients from domestic wastewater.

2.9 Operation conditions

The operation conditions of different experimental set ups are given in Table 2.

Table 2: Operation conditions of different experimental set up

Operation conditions of experimental set ups		
Auto controlled cross flow set up	**Manually controlled cross flow set up**	**MBR**
Test media: HA dissolved in distilled (DI) water Concentration: 100 mg/L Conductivity of feed solution: 60 µS/cm pH: 6.5-7 Temperature: 20 ± 2°C TMP: 0.5±0.02 bar Operation time: 24h Active surface area of the used membrane: 86 cm^2	Test media : MTDW pH: 7.5 ± 0.5 Temperature: 22 ± 2°C TMP: 3.0±0.50 bar CFV: 1 L/min. Operation time: 2 h Active surface area of the applied membrane: 80 cm^2	Test media: RTW pH: 8 ± 0.2 Temperature:25 ± 2°C TMP: 70-350 mbar Operation time: 150 days Active surface area of the applied membrane: 0.34 m^2 for PES-MBR and 0.31 m^2 for PBM-MBR

2.10 Analytical methods for model textile wastewater

All COD were analysed with COD cell tests (Model: 1.14541 Merck KGaA, Germany). The concentrations of red and blue dyes were determined using a spectrophotometer (Model: UV-1800; Shimadzu, Japan) using Beer's law at wavelengths of 505 nm and 595 nm respectively. Oxygen sensor (Model: Oxi340i meter and cellOXs 325 O2 electrode; WTW, Germany) was used to measure the dissolved oxygen, pH and temperature values were measured with pH meters (Model: pH 323 and Sentixs 41-3 electrode) integrated with temperature sensors

(WTW GmbH, Germany). Conductivity measurements were conducted with a conductivity meter (Model: Cond 315i meter; WTW). All AFM measurements were performed with a Multimode AFM with Nanoscope IIIa controller (Veeco, USA) using manufacturer supplied software. Tapping mode measurements in air were performed using TESP (nominal spring constant 20-80 N/m) cantilevers (Bruker AXS).

2.11 Analytical methods for industrial textile wastewater

Conductivity and pH determinations were performed by means of a conductimeter, CONSORT C 831 model and pH meter, Istek-NeoMet respectively. Soluble COD was estimated as described by Knechtel [32]. Mixed liquor suspended solids (MLSS) was measured as the standard method for examination of water and wastewater [33]. Colour was measured by spectrophotometric absorbance using UV–visible spectrophotometer (Perkin Elmer Lambda 20 UV/VIS Spectrophotometer) at a wavelength of 620 nm in which maximum absorbance spectra was obtained. Dye decolourization was determined by monitoring the decrease in the absorbance peak at the maximum wavelength for the global effluent.

3. Results and discussion

3.1 Microemulsion phase diagram and conductivity measurements

Fig. 3 shows the pseudoternary phase diagram made. A phase diagram can be proposed as a useful tool for the determination of the single phase region when oil, water and a surfactant are mixed together. Each corner of the triangle represents 100% of that respective component. For the formulation of microemulsions, generally, a co-surfactant (usually represented by a short-chain alcohol) is applied in order to widen the microemulsion single phase region [34].

The co-surfactant is an amphiphilic molecule having affinity for both the aqueous phase and oil phase contributing, along with the surfactant, to decrease the interfacial tension. Among the whole range of possible compositions, it can be noticed that not every combination of the components led to the production of a microemulsion. In particular, the shaded area (in grey) in Fig. 4 represents the area where microemulsions can be formed. The addition of the co-surfactant, HEMA certainly promoted the enlarging of the phase region by increasing the flexibility of the interfacial film [35].

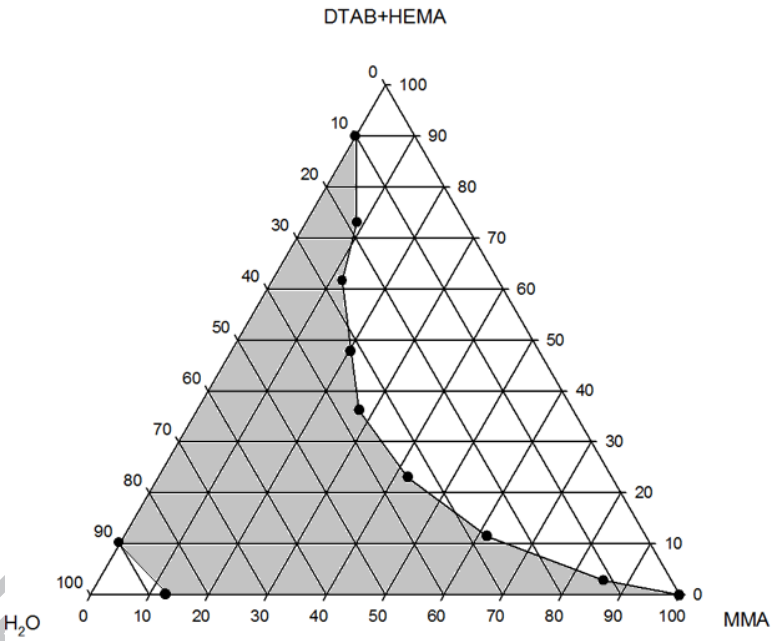

Fig. 3. The pseudoternary phase diagram with microemulsion region (grey area)

The variation of conductivity as a function of DTAB aqueous solution is shown in Fig. 4. Conductivity measurements were carried out in order to differentiate the three types of microemulsions: W/O (water in oil), O/W (oil in water) and bicontinuous microemulsions. The bicontinuous microemulsion range is generally associated with a sharp increase in conductivity values [35] and can be identified in the range between 20% and 90% DTAB aqueous solution content. Below and beyond this range, W/O and O/W microemulsions can

be formed respectively. The same trend in conductivity has been already observed by Chieng et al. [36] when DTAB was used as a surfactant for microemulsion preparation.

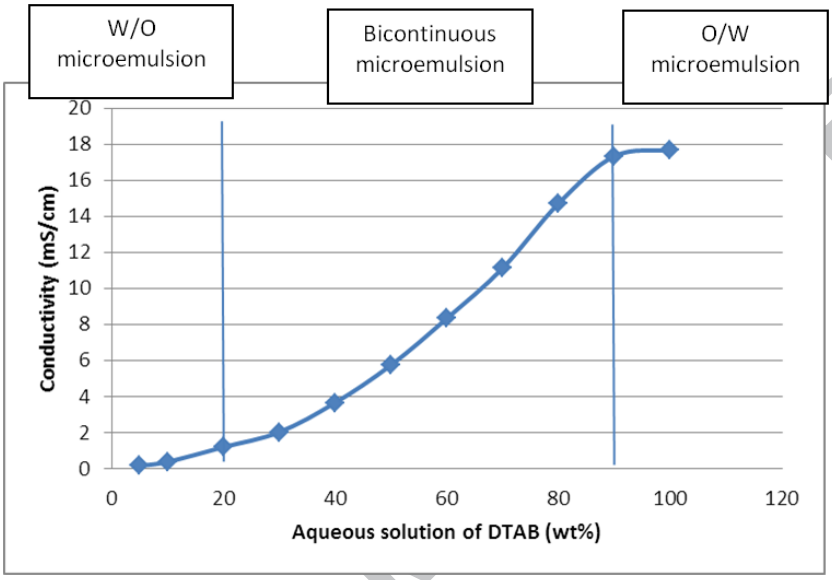

Fig. 4. The variation of conductivity of the microemulsion system as a function of aqueous solutions of DTAB

3.2 Preparation of PBM membranes

For the preparation of PBM membranes, as pre-screening, the concentration of HEMA (from 35 to 50 wt%) and the polymerization temperature (from 30 to 50°C) were varied in order to evaluate their effect on the permeability and the dye rejection. Produced membranes were identified with the codes A-E and reported in Table 3. The different compositions of each microemulsion prepared were selected on the basis of the results of pseudoternary phase diagram (for the identification of the microemulsion range) and of conductivity measurements (for the identification of the bicontiunuous structure).

Table 3: HEMA concentration and polymerization temperature (Tp) for the PBM membranes prepared

MEMBRANE CODE	HEMA CONC. (wt%)	POLYMERIZATION TEMP., Tp (°C)
A	40	20
B	35	30
C	50	20
D	50	25
E	50	30

3.3 Weight loss determination

The quantity of unreacted material in the PBM membranes was determined by evaluating the weight loss after different extractions to which the membranes were exposed.

The water weight loss after drying the membrane in the oven was of about 7 wt%. After toluene extraction, the membrane weight loss was null indicating that the whole MMA and HEMA were fully copolymerised within the polymeric matrix. After hot water extraction, PBM membranes presented a weight loss of about 16 wt% due to the fact that, as expected, the non-polymerisable DTAB surfactant was washed away from the membrane matrix.

3.4 Morphological analysis: SEM

When compared to PES uncoated surface (Fig. 5), PBM membranes presented the typical bicontinuous structure [25] made up of an interconnected network of polymer channels (white strips) and water channels (dark strips) (Fig. 5 A-E). As can be observed in SEM images, the

polymerised bicontinuous structure is clearly visible at magnifications of x 20 000 and higher and has a surface structure significantly divergent from that of the untreated PES membrane. The PBM surface appears uniform and homogenous with a random distribution of the bicontinuous structure. This appearance is typical of the surface structure previously reported for other PBM coated membrane surfaces produced by using the alternative surfactant acryloyloxyundecyltriethylammonium bromide (AUTEAB) [25, 37]. The coating thickness, determined by SEM cross-sections, was about 2-5 µm.

The polymerization temperature seems to play an important role in the formation of the final PBM morphology. In fact, by increasing the polymerization temperature (from 20 to 30°C) the water channels (representing the porous region of the membrane) are gradually replaced by the white islands (representing the polymer aggregates) as can be, for instance, observed for the samples C, D and E (prepared at 20, 25 and 30°C respectively and at constant HEMA concentration) and showed in Fig. 5. This phenomenon was already observed and reported by Ming et al. [38] for the polymerization of polymethyl methacrylate (PMMA) and explained as an higher aggregation of polymer particles at higher temperatures (see also section 3.6.1). Also, the increase of HEMA concentration (from 35 to 50 %) led to a decrease of membrane porosity, as can be observed for samples B, A and E (prepared with 35, 40 and 50 wt% respectively of HEMA concentration and at constant temperature) due to its narrowing effect in bicontinuous microemulsion systems [39].

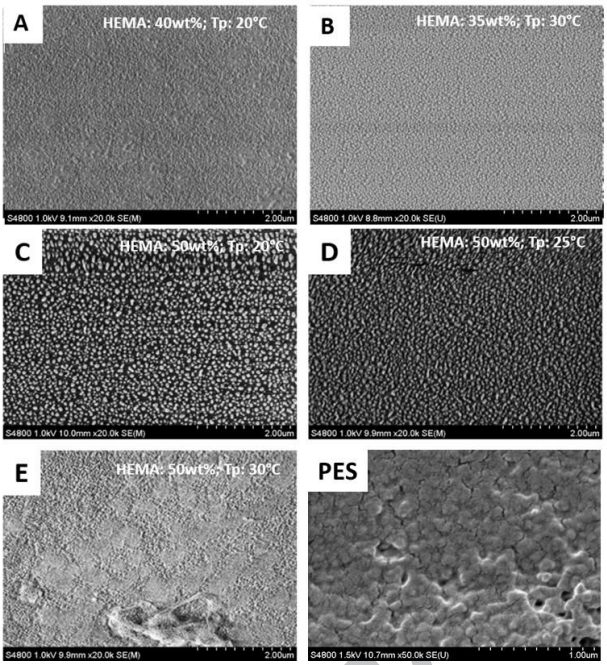

Fig. 5. SEM surface of PBM membrane surfaces A-E, varying the HEMA concentration and Tp and PES commercial membrane

3.5 Surface analysis: AFM, CAM and FT-IR

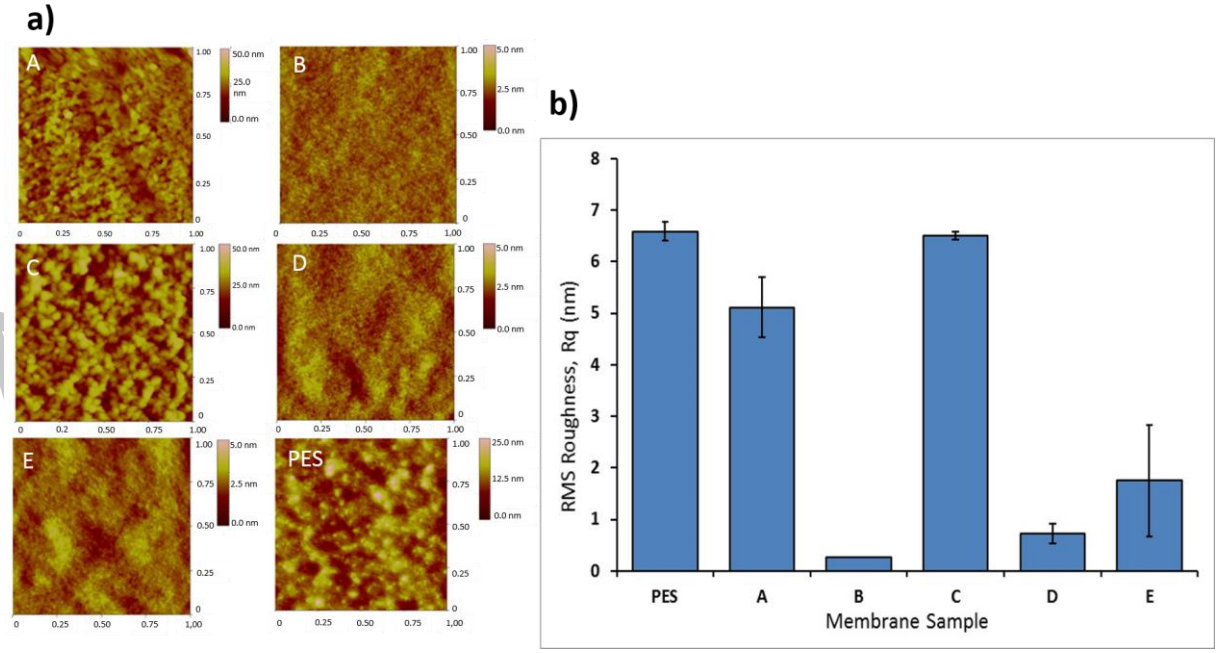

Fig. 6. a) 1x1 µm AFM surface scans of PBM membranes. Images are labelled according to the sample key in Table 3. b) Root mean squared (Rq) roughness for PES and PBM

membranes from 1x1 µm AFM scans. Error bars indicate standard error of the mean. Samples are labelled according to the key in Table 3.

AFM scans were carried out using tapping mode in air (Fig. 6a). From the AFM topographies, roughness parameters were calculated for several PBM membranes prepared at a range of HEMA concentrations and polymerization temperatures and compared with surface roughness values obtained from the unmodified commercial PES membrane. Fig. 6b shows the root mean square (Rq) values obtained for each membrane obtained from an average of three scans at different portions of the membrane surface. All scans were of a 1 x 1 µm size. Membranes are coded A-E and Table 3 provides a key to the coding. As can be seen the unmodified PES membrane has an Rq value of 6.59 nm. Rq values for the PBM membranes vary from comparable with the PES membrane (membranes C) to having significantly lower surface roughness at this size scale for the remaining membranes.

Roughness can play a critical role in the surface fouling of membranes as it changes the amount of surface area available for fouling to occur. Much effort has been made into combating surface fouling by fabricating smoother membranes, as many observations have been reported in the literature that higher surface roughness can lead to increased fouling by increasing the interaction area between dissolved and suspended foulants and the membrane [40]. However, the effect of roughness on fouling is complex, and can depend on the interplay between roughness, foulant particle size and surface morphology [41, 42]. Many researchers have found a strong correlation between fouling and surface roughness [43]. For example, cellulose acetate membranes are generally more resistant to fouling than rougher polyamide membranes [44], which has been in part attributed to lower shear rates over rougher surfaces [45]. Rana et al. [46] reported a linear correlation between fouling induced flux reduction and surface roughness for modified and unmodified PES membranes.

From CAM measurements, PES commercial membranes presented an average contact angle of 68° ± 3 while PBM membranes presented a contact angle ranging from 44° to 55°. The surface roughness in this case can not be related to the phenomenological model proposed by Wenzel [47] where the increase of surface roughness generally corresponds to an increase in membrane hydrohilicity. However, other models have been also studied and proposed putting in relation the membrane roughness with membrane contact angle based upon the triple contact line (TCL), as illustrated in the works of Liu et al. [48, 49], giving20n the possibility of having a fundamental understanding of wetting of rough and heterogeneous substrates.

Besides membrane roughness, it is important to consider the contribution of the co-surfactant HEMA which, being a short-chain alcohol, bears –OH functional groups able to improve the affinity of the PBM coated membrane toward water molecules and decreasing, therefore, the contact angle value.

FT-IR measurements were aimed in determining the effective presence of the PBM coating on PES membrane surface and its stability once the PBM membrane was subjected to different washing protocols. As can be seen from Fig. 7, showing the spectra of the PBM and PES membrane, the presence of the relative broad absorption at 1725 cm^{-1} in the PBM membrane, clearly indicates the presence of the carbobyl group characteristic of MMA, HEMA and EGDMA molecules used for the coating preparation. The same functional group was still present after the different washing procedures carried out on the PBM membrane, evidencing the stability of the coating on the PES membrane surface.

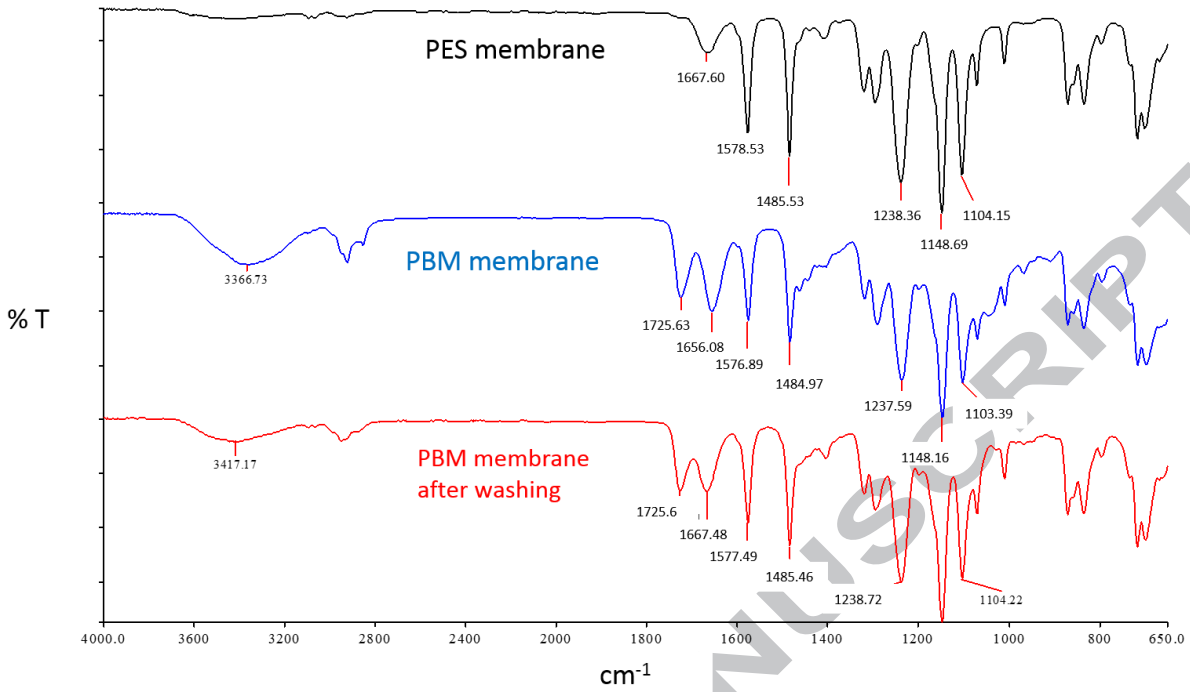

Fig 7. FT-IR spectrum of PES and PBM membrane (before and after washing)

3.6 Lab scale experiments

3.6.1 Effect of microemulsion composition and polymerization temperature on membrane performances

The microemulsion composition can have a significant impact on membrane formation leading to structures with a more open/closed morphology. For this reason, several sets of novel PBM membranes were prepared following the preparation method described in section 3.3 under different polymerization temperatures i.e. from 20° C until 30° C and HEMA concentration ranging from 35% to 50%. The water permeabilities (WP) and dye rejections obtained from the manually controlled cross flow set up (Fig. 1) are given in Fig. 8 (a, b).

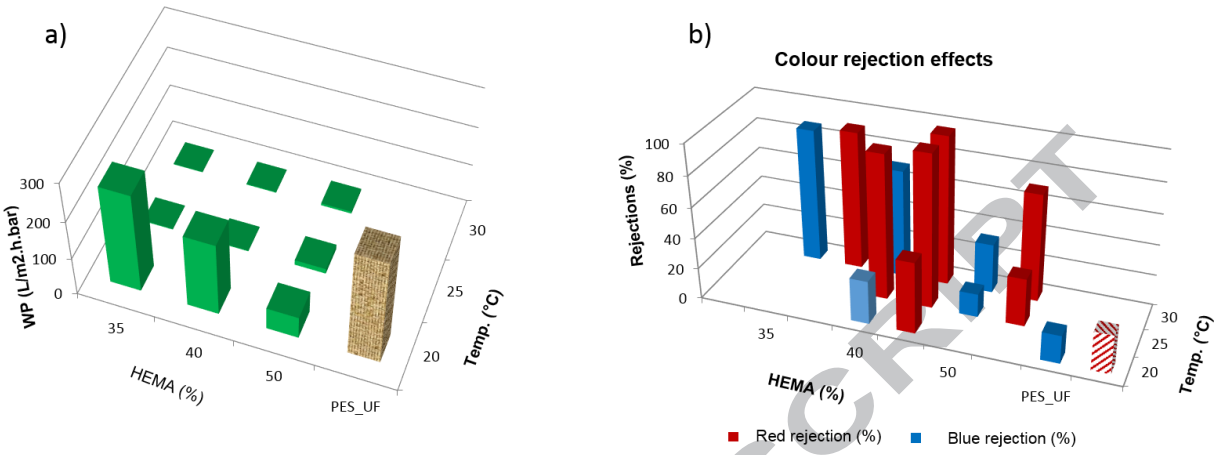

Fig. 8. Water permeability a) and b) colour rejections of the novel PBM membranes

From Fig. 8 (a) it can be observed that the water permeability of the evaluated membranes decreases with an increase in the reaction temperature.

An explanation of this behavior lies in the fact that the reaction temperature can play a crucial role in the determination of particle size and in the subsequent formation of membranes with a more or less porous architecture. Ming et al. [38], in fact, demonstrated how the increase of polymerization temperature of PMMA led to an increase of latex particle size in comparison to systems polymerized at room or lower temperatures. Higher temperatures, in fact, can foster the diffusion of MMA into the polymer-containing particles and, at the same time, facilitate the collision and aggregation of polymer particles to form larger latex particles.

The increase of latex particles at higher temperatures, therefore, could have promoted the formation of denser membranes due to the occlusion of the water channels by the growing polymer particles causing a drastic decrease in membrane water permeability. Moreover, the increase in HEMA concentration from 35 to 50 wt% presented in Fig. 8 (a), negatively influenced the water permeability of the prepared membranes. Due to its high solubility in water, the co-surfactant HEMA localizes not only at the interface of MMA and water, but also in the water channels of the bicontinuous microemulsion [39]. The presence of HEMA

and its copolymers in the water channels is, thus, able to narrow the pores of the membranes [50], causing a decrease of water permeability and a consequent increase of dye rejection. These results are also in agreement with the different morphology exhibited by PBM membranes when observed by SEM. The dye rejection (Fig. 8 (b)) reflects the trend of water permeability. Membranes prepared at higher temperatures (30°C) presented the highest rejection due to their closer and denser structure. For these reasons, the membrane fabricated with 40 wt% of HEMA and 20 °C was selected as the best compromise between permeability and rejection and, therefore, chosen as optimal conditions for the following antifouling tests with HA and with real textile wastewater in MBR process. This particular membrane treatment had a lower roughness than the unmodified PES membrane (membrane A in fig. 5, 6a, 6b).

3.6.2 Antifouling tests

To test the fouling propensity of the membranes, HA was used as a model foulant using the operating conditions in Table 2. The experiment performed with model foultant HA showed that water permeability (WP) with PES membrane reduced to 78% (from 638 L/m^2 h bar to 140 L/m^2 h bar on average), while the reduction of WP with PBM membrane was only 35% (from 73 L/m^2 h bar to 47 L/m^2 h bar on average), Fig. 9 (a). The results indicate that the novel PBM membrane is less prone to fouling by organic substances than the unmodified commercial membrane.

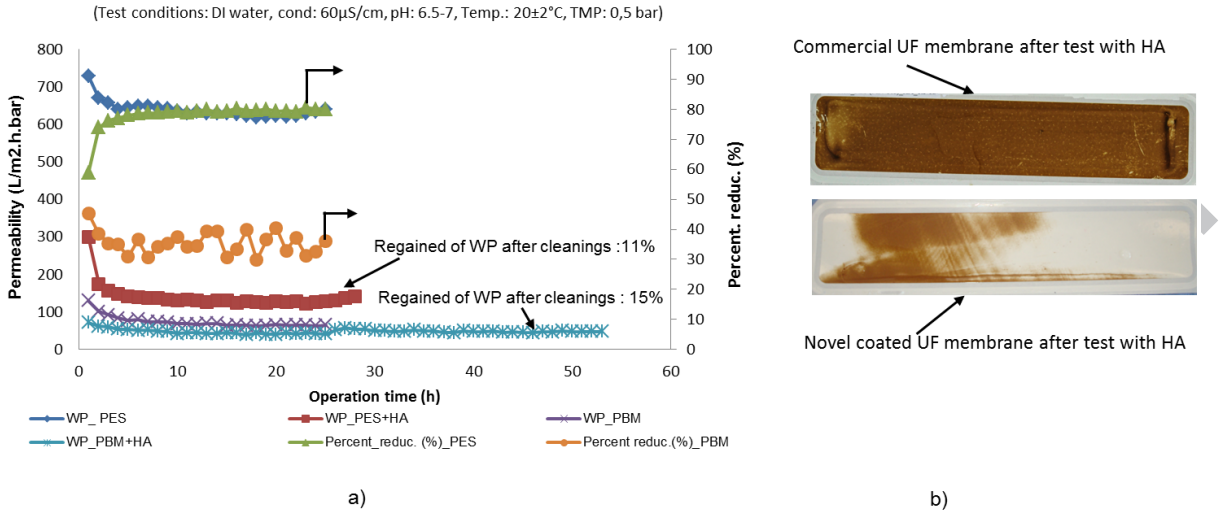

Fig. 9. a) Water permeability (WP) and b) fouling behaviour of the novel membrane in comparison to PES commercial one

WP regained after the 3rd cleaning operation was approximately 15% for the PBM membrane while it was approximately 11% for pristine PES membrane. WP gain indicates the fouling reversibility and therefore the removal of HA with DI water from the membrane surface. If it is assumed that 78% WP loss of PES membrane is caused by the total fouling (reversible and irreversible), while the contribution of reversible fouling is only 11% and the rest (67%) represents the irreversible category. Considering a similar hypothesis, PBM membrane showed almost 15% reversible fouling after 3 cleaning cycles with DI water whereas the rest (20%) falls into the irreversible catagory. This is a further indication of the low fouling effect of the PBM membrane is mainly related to reversible fouling. The physical appearance for both membranes after 3 cleaning cycles also indicates the different affinity of model foulant to the membrane surfaces (Fig. 9 (b)), showing that HA has less affinity to PBM membrane compared to PES. The lower tendency of PBM membranes to be affected by fouling in comparison to PES commercial membranes can be attributed to two main causes: the smoother surface and the superior hydrophilicity of the novel membranes. Membrane roughness plays an important role in the formation and evolution of membrane fouling at the

surface. Surface roughness, in fact, enhances the attachment of fouling particles on the membrane surface as already pointed out by many authors [51, 52, 45]. Rough surfaces are able to offer a wider surface area and more contact opportunities between the foulants and the membrane surface [44]. Moreover, the troughs created by rough membranes are preferred sites of particle accumulation in comparison to smoother surfaces. However, it should be noted that the particular membrane used for membrane fouling tests was not smoother to a great degree, so roughness can only partly explain the lower fouling behavior of this particular membrane. The higher degree of hydrophilicity exhibited by PBM membranes further contributed to the lower fouling propensity of the coated membrane in comparison to the commercial one. Hydrophilic surfaces are, in fact, considered more resistant to fouling phenomena because organic matters in aqueous media tend to be hydrophobic having, thus, higher propensity to establish hydrophobic interactions with the surface of hydrophobic membranes [53-55].

3.7 Pilot scale experiment with real textile wastewater

In Table 4 the main characteristics of sampled RTW are summarized.

Table 4: Characteristics of RTW

RTW	**pH**	**EC (mS/cm)**	**COD (mg/L)**	**BOD_5 (mg/L)**	**TSS (g/L)**	**VSS (g/L)**
1	12	15.01	2880	350	2.35	0.59
2	12.2	9.11	1946	1050	0.63	0.05
3	7.3	5.36	3120	1200	0.2	0.1

The effluent used to feed the MBRs presented high pH values added to relatively high salinity. Such conditions are not favourable for the microbial activity. Therefore, the effluent was diluted prior to MBR feeding and the pH was adjusted to 8 in order to ensure maximal biological activity.

3.7.1 Effect of pH and salinity on MBR

pH is an important parameter in biodegradation and membrane fouling too. It has been reported that the rate of membrane fouling is strongly influenced by low pH values thus increasing the adsorption of MBR originated EPS onto the membrane [56]. In this context, many studies approved that the rate of membrane fouling in MBRs increases at lower pH of the mixed liquor [57, 58]. Even though pH between 8 to 9 increases the precipitation of $CaCO_3$ [59], moderate amounts of calcium precipitates can be beneficial in controlling biofouling due to the bounding and bridging EPS hence enhancing biofloculation. In order to avoid fouling, alkalinity is required to buffer the hydrogen ions generated in MBR processes [60]. On the other hand, many studies have previously reported that bacterial culture generally exhibits maximum decolourisation at a neutral or a slightly alkaline pH value [61]. On the basis of these reports, the optimum pH for running the MBR operation was about 8.

Regarding the salinity, it has been known to have adverse effects on biological systems. In MBRs particularly, it has been demonstrated that the presence of salts in the mixed liquor cause chemical precipitation and electrostatic attraction towards the surface of the membrane [62]. High salinity also modifies the physical and biochemical properties of the biomass characteristics by increasing bound EPS and SMPs concentrations and decreasing membrane permeability [63]. In our case, the feed presented normal salinity content below 5000 mg/l and there was no salt accumulation in both MBRs. It is worth noting that salt concentrations below 10 g/L had negligible impact on the removal of organics by MBR [64, 65]. Thus, suggesting the biomass adaptation to the salinity condition [66]. Similarly, salinity and pH of

the wastewater did not affect the performance of both MBRs as the resulting permeates revealed comparable salt content with mean values of 4420 and 4410 mg/l for uncoated and coated PBM membranes, respectively.

3.7.2 Performance comparison of commercial membranes and PBM membranes on COD removal

The MBRs were started with a low mean COD load of 0.7 g COD/L/day to let the biomass adapt to the operational conditions during the first two months. After the adaptation phase, the volumetric loading rate (VLR) was increased stepwise to 2 g COD/L/day. The sludge concentration increased from 5 to 14 g/L and was kept at almost 12 g/L for the rest of the MBR operations by periodical sludge withdrawal.

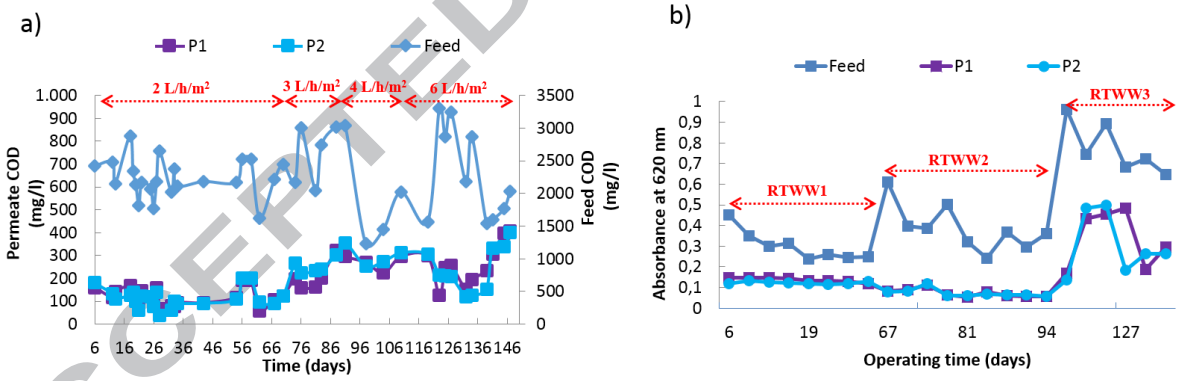

Fig. 10. a) Evolution of COD removal performance during MBR treatment: (P1) permeate of PES-MBR; (P2) permeate of PBM-MBR. b) Evolution of colour removal performance during MBR treatment: (P1) permeate of PES-MBR; (P2) permeate of PBM-MBR.

As shown in Fig. 10a, during the first operational period where a flux of 2 L/h/m^2 and a VLR of 0.7 g COD/l/day were applied, PES-MBR and PBM-MBR exhibited COD removal

efficiencies of 94.6% and 94.9%, respectively. At higher flux of 4 L/h/m2 (VLR 1 g COD/L/day) both MBRs showed a stable performance with a slight decrease in COD removal efficiency recording values of 84.6% and 83.4% for PES- PBM and PBM- MBR, respectively. Further flux increase (6 L/h/m2) associated with a VLR of 2 g COD/L/day resulted in a better COD removal performance of 87.3% and 88.1% for PES- PBM and PBM-MBR. The general assessment of the data shows that both reactors exhibited similar performances.

3.7.3 Performance comparison of commercial membranes and PBM membranes on colour removal

To study the performance of the commercial membranes and PBM membranes on colour removal throughout the continuous treatment process, the colour of influent and effluent was assessed through absorbence at 620 nm.

Table 5. Operating conditions of the MBRs at different stages of the experiment

HRT (days)	3	2.5	1.7	1.2
Flux (L/m^2 h)	2	3	4	6
Decolourization (%)				
PES MBR	63.5	78.3	82.4	51.4
PBM MBR	67.0	78.4	83.0	51.0

At the start up of both MBRs (flux 2 L/h/m^2, HRT 3 days), colour removal was 63.5% and 67.0% for PES-MBR and PBM-MBR, respectively (Table 5). Beyond this adaptation phase,

applying a HRT of 2.5 days and a flux of 3 L/h/m^2 resulted in higher colour removal values reaching 78.3% for both MBRs (Table 5). Additional flux increase (flux 4 L/h/m^2) and HRT reduction (1.7 days) induced higher colour removal with mean values of 82.4% and 83.0% for PES-MBR and PBM-MBR, respectively (Table 5). This suggests the adaptation of the biomass to the operating conditions allowing the improvement of the decolourization rate even at reduced HRT.

In order to improve the membrane performances, the flux was increased to 6 L/h/m^2, and the resulting HRT was almost 1 day. Following this change, the decolourization performance decreased to 51.4% for PES-MBR and 51.0% for PBM-MBR (Table 5). Obviously, the HRT together with the change of the effluent fed to the MBRs affected the permeate quality becoming progressively more coloured for both MBRs (Fig. 10b). It can be concluded that the minimum appropriate HRT for such complex wastewater is 1.5-2 days. The comparison of the PBM coated membranes vs. the commercial membranes in terms of decolourization revealed that both membrane performances were also quite similar.

3.7.4 Fouling propensity of commercial membranes and PBM membranes during MBR treatment

Fig. 11 displays the TMP variation of PES- MBR and PBM- MBR at different permeate flux. Results showed that both membranes were stable under flux below 5 L/h/m^2 as the maximum observed TMP values was 50 mbar after almost 120 days of continuous treatment (Fig. 11).

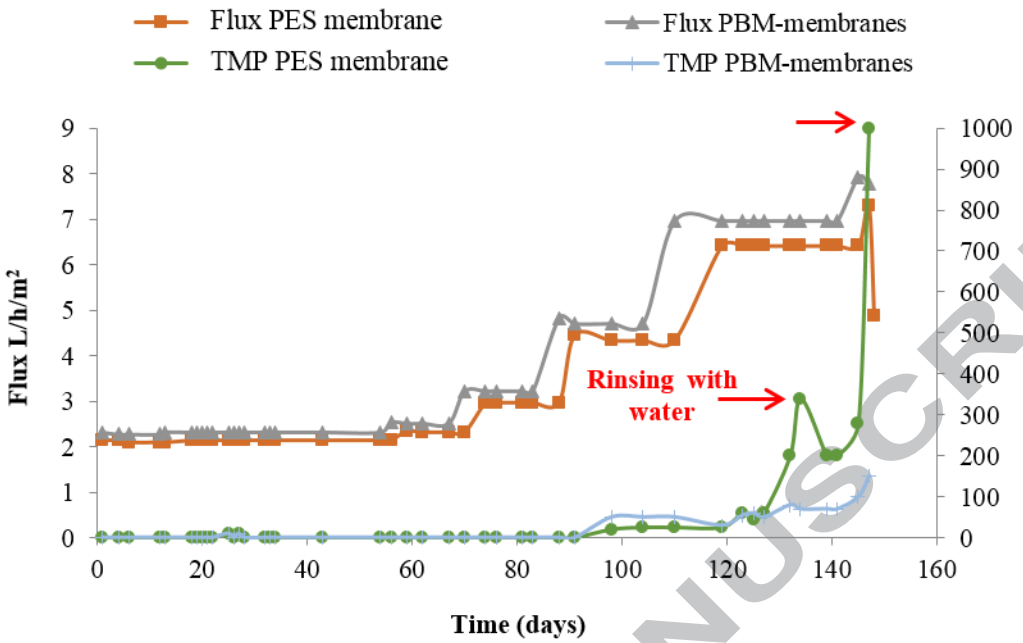

Fig. 11. Course of TMP and Flux during the entire operation period of PES-MBR and PBM-MBR

Increasing permeate flux up to 6-7 L/h/m^2 led to the rise of TMP values reaching 340 mbar at day 134 for commercial membranes against 70 mbar for PBM membranes (Fig. 11). Consequently, the commercial membrane module was extracted from PES- MBR and jet rinsed with tap water. The TMP regained 200 mbar at day 139 (Fig. 11). However, the positive effect of rinsing lasted too short (8 days) and a strong membrane fouling was observed as TMP values drastically increased up to 1 bar (Fig. 11). Unlike the commercial membranes, PBM membranes showed steady filtration performance under the same flux with TMP values not exceeding 150 mbar (Fig. 11).

Pictures of both membranes were taken at the end of the trials before and after the water rinsing and are showed in Fig. 12. As it possible to notice, PBM membranes visually appeared much less fouled after MBR trial in comparison to PES ones. Moreover, the water rinsing for PBM membranes was more efficient in removing the deposited fouling facilitating the

permability restoring. Considering these results, the PBM coating of the membranes lowered the tendency to fouling in comparison to the commercial membranes.

According to the membrane producer of the pristine PES membranes, the lifetime of the membrane is around 5 years if the operation protocol is maintained carefully. However, its lifetime could be reduced drastically if the membrane faces fouling. From the antifouling test (lab test) of uncoated membrane, as described in section 3.6.2, and pilot tests, as described in section 3.7.4 (Fig. 11), it is evident that the coated membrane is less prone to fouling which ensures the much longer life time and making the PBM coating a very promising approach.

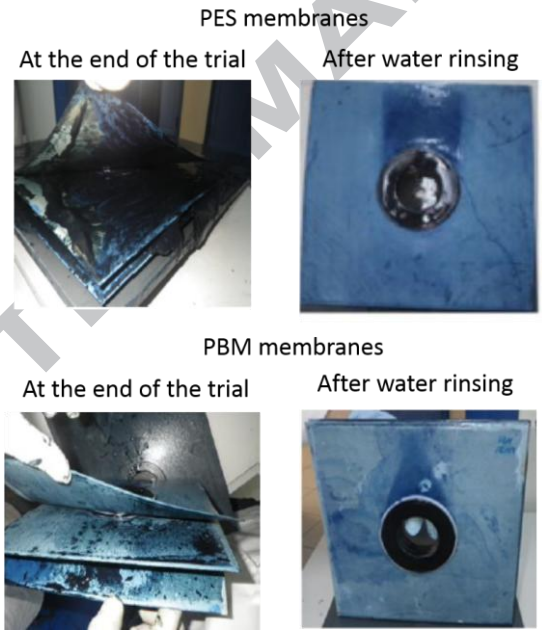

Fig. 12. PES and PBM membranes after MBR trial and after rinsing with water

3.7.5 Comparison between PBM membranes prepared with AUTEAB and DTAB

The result of the present work has been compared with other two studies in which the PBM membrane concept has been developed for water treatment [15, 25]. The PBM membranes produced typically differ for the use of a specific surfactant: lab-made and polymerisable surfactant AUTEAB in case of the previous studies; and commercial not-polymerisable

DTAB surfactant in case of the present work. In table 6 a comparison between PBM membranes main characteristics and performances, prepared with AUTEAB and DTAB surfactants, is reported. In particular, the main difference between the two types of PBM membranes lies in the type of surfactant used. The lab-made surfactant AUTEAB is, in fact, an anti-microbial and polymerisable molecule, which remains entrapped, through co-polymerization, in the PBM matrix upon polymerization. This gives to the overall PBM membrane important anti-biofouling properties when operated in MBR process. DTAB surfactant, despite its anti-microbial activity, however, is not a polymerisable molecule. For this reason it cannot be chemically entrapped in the PBM membrane during the polymerization process and it cannot exploit any anti-biofouling activity due to its release during membrane washing. Nevertheless, PBM membrane coating prepared with DTAB allow to fabricate a bicontinous microemulsion structure with similar performance, in terms of water permeability, COD removal efficiency in MBR and low fouling properties (when tested with HA), in comparison to PBM prepared with AUTEAB. From the cost point of view, PBM membranes prepared with DTAB are slightly cheaper due to its commercial availability.

Table 6. Comparison between PBM membrane main characteristics and performances

	PBM membranes main characteristics	PBM membrane performances	Cost	

** Costs of chemicals ordered for lab scale synthesis.*

	Polymerisable surfactant	Antimicrobial and anti-biofouling activity after polymerization	Tunable pore size	Smoother surface	Water permeability (L/m^2 h bar)	Permeability reduction when HA is used as foulant (%)	COD removal efficiency in MBR (%)	Cost* of PBM coating per 1 m^2	References
PBM with AUTEAB	Yes	Yes	Yes	Yes	200 ± 75	45 ± 3	95 ± 1	~ 47,00 €	[15, 25, 67]
PBM with DTAB	No	No	Yes	Yes	192 ± 50	35 ± 4	94.9 ± 1	~ 41,00 €	This work

4. Conclusions

In this work, PBM membranes, applied as a coating material for PES ultrafiltration membranes, have been obtained through the polymerization of a bicontinuous microemulsion. The new coating has been realized using commercially available dodeyltrimethylammammonium bromide (DTAB) as surfactant and by varying the chemical composition and the polymerization temperature of the microemulsion. The microemulsion region and the bicontinuous range were determined by phase diagram and conductivity measurements, respectively. Different PBM membranes were successfully produced tailoring the different properties in terms of morphology allowing a change in water permeability and dyes rejection (when tested in model textile wastewater). The concentration of the co-surfactant HEMA of 40 wt.% and the polymerization temperature (Tp) of 20 °C have been selected as the optimal conditions in terms of water permeability (WP) and dye rejection for the scale up of PBM membranes. PBM coating presented interesting properties in terms of antifouling resistance (when tested with HA) in comparison to PES uncoated membranes. The fouling occurring in PBM membranes, in fact, was mainly of the reversible type, allowing a higher regain in WP after flushing with water. The MBR pilot scale experiments, carried out with real textile wastewater, showed that critical flux was significantly higher for the novel PBM coated membranes with respect to the commercial PES membranes resulting in a longer life cycle of the produced membranes with less requirements in terms of chemical cleaning and operational maintenance costs.

Acknowledgements

This paper presents findings of an EU funded project “Development of the next generation membrane bioreactor system (BioNexGen, 2013) which aims at developing novel functionalized low-fouling membranes for membrane bioreactors (MBRs) in wastewater

treatment. The European Commission is gratefully acknowledged for the financial support of the BioNexGen project under grant agreement no. CP-FP 246039.

References

[1] S. Judd, in: The MBR Book: Principles and applications of membrane bioreactors in water and wastewater treatment, 2nd Ed., London, 2011, Elsevier.

[2] M. Simonic, Text. Light Ind. Sci. Technol. 2 (2013) 71-77.

[3] N. Abidi, E. Errais, J. Duplay, A. Berez, A. Jradi, G. Schafer, M. Ghazi, K. Semhi, M. Trabelsi-Ayadi, J. Clean. Prod. 86 (2015) 432-440.

[4] P. Baskaralingam, M. Pulikesi, V. Ramamurthi, S. Sivanesan, , Appl. Clay Sci. 37 (2007) 207-214.

[5] F. Yuzhu, T. Viraraghavan, 79 (2001) 251-262.

[6] C. I. Pearce, J. R. Lloyd, J. T. Guthrie, Dyes Pigments 58 (2003) 179-196.

[7] B. Van der Bruggen, E. Curcio, E. Drioli, J. Environ. Manage. 73 (2004) 267-274.

[8] J. Porter, Wastewater treatment in the textile industry, In: Treatment of Wastewaters from Textile Processing. TU-Berlin Schiftenreihe biologische Abwasserreinigung, 9 (1997) Berlin.

[9] R. Minke, U. Rott, Innerbetriebliche anaerobe Behandlung organisch hoehbelasteter und stark farbiger Teilstromabwasser der Textilveredelungsindustrie, in: Preprints, Colloquium Produktionsintegrierte Wasser-/Abwassertechnik, Naeh_haltige Entwicklung in der Textilveredlung (1997) Bremen.

[10] R. Minke, U. Rott, Prozesswasserrückgewinnung und Abwasservorbehandlung bei der Garnveredelung. Preprints des Colloquium Produktionsintegrierte Wasser-/ Abwassertechnik

"Nachhaltige Entwicklung in der Textilveredelung und Membrantechnik" vom 17.-18 (2001) Bremen, Seite B 129 - B 142.

[11] A. Lopez, G. Ricco, R. Ciannarella, A. Rozzi, A. C. Di Pinto, R. Passino, Water Sci. Technol. 40 (1999) 99-105.

[12] A. Rozzi, R. Bianchi, J. Liessens, A. Lopez, W. Verstraete, W., Ozone, Granular activated carbon and membrane treatment of secondary textile effluents for direct reuse, In: Treatment of Wastewaters from Textile Processing, TU-Berlin Sehiftenreihe biologisehe Abwasserreinigung, 9 (1997) Berlin.

[13] M. Marcucci, G. Nosenzo, G. Capannelli, I. Ciabatti, D. Corrieri, G. Ciardelli, Desalination 138 (2001) 75 – 82.

[14] G. Braun, O. W. Felgener, Treatment of Wastewaters from Textile Processing. TU-Berlin Schiftenreihe biologische Abwasserreinigung, 9 (1997) Berlin.

[15] A. D. Deowan, F. Galiano, J. Hoinkis, D. Johnson, S. A. Altinkaya, B. Gabriele, N. Hilal, E. Drioli, A. Figoli , J. Membr. Sci. 510 (2016) 524–532.

[16] T. Reemtsma, B. Zywicki, M. Stueber, A. Kloepfer, M. Jekel, Environ. Sci. Technol., 36 (2002) 1102-1106

[17] G. Laera, D. Cassano, A. Lopez, A. Pinto, A. Pollice, G. Ricco, G. Mascolo, Environ. Sci. Technol. 46 (2012) 1010-1018

[18] S. Krause, P. Cornel, Aeration energy demand in municipal MBRs, International Conference on Membrane Bioreactors MBR4, Cranfield University (2003) ISBN: 1861940068.

[19] J. A. Howell, H. C. Chua, T. C. Arnot, J. Membr. Sci. 242 (2004) 13-19.

[20] T. Jiang, M. D. Kennedy, W. G. J. van der Meer, P A. Vanrolleghem, J. C. Schippers, Desalination 157 (2003) 335-343.

[21] G.D. Bella, G. Mannina, G. Viviani, J. Membr. Sci. 322 (2008) 1–12.

[22] A. Zarragoitia-Gonza´ lez, S. Schetrite, M. Alliet, U. Ja´ uregui-Haza, C. Albasi, J. Membr. Sci. 325 (2008) 612–624.

[23] C. Suh, S. Lee, J. Cho, Investigation of the effects of membrane fouling control strategies with the integrated membrane bioreactor model, J. Membr. Sci. 429 (2013) 268–281.

[24] A. Figoli, J. Hoinkis, B. Gabriele, G. De Luca, F. Galiano, S.A. Deowan, Bicontinuous Microemulsion Polymerized Coating for Water Treatment, patent WO 2015044335 A2 (2016).

[25] F. Galiano, A. Figoli, S. A. Deowan, D. Johnson, S. A. Altinkaya, L. Veltri, G. De Luca, R. Mancuso, N. Hilal, B. Gabriele, J. Hoinkis, J. Membr. Sci. 482 (2015) 101-114.

[26] F. Galiano, S. A. Schmidt, X. Ye, R. Kumarb , R. Mancuso, E. Curcio, B. Gabriele, J. Hoinkis, A. Figoli, Sep. Purif. Technol. 194 (2018) 149-160.

[27] X. Lu, Y. Peng, H. Qiu, X. Liu, L. Ge, Desalination, 413 (2017) 127-135.

[28] C. Liu, J. Lee, C. Small, J. Ma, M. Elimelech, J. Membr. Sci., 544 (2017) 135-142.

[29] A. Y. Kirschner, C.-C.Chang, S. Kasemset, T. Emrick, B. D. Freeman, J. Membr. Sci. 541, (2017) 300-311.

[30] E. Igbinigun, Y. Fennell, R. Malaisamy, K. L. Jones, V. Morris, J. Membr. Sci., 514 (2016) 518-526.

[31] I. Sutzkover-Gutman, D. Hasson, R. Semiat, Desalination 261 (2010) 218–231.

[32] R. J. Knechtel, J. Water Pollut. Control (1978) 25-29.

[33] A. E. Greenberg, L. S. Clesceri, A. D. Eaton, Method 6210 volatile organics, purge and trap gas chromatographic/mass spectrometric method, standard methods for the examination of waste and wastewater, Eighteenth Edition, American Public Health Association, Washington, DC, 1992.

[34] M. J. Lawrence, G. D. Rees, Adv. Drug Delivery Rev. 64 (2012) 175–193.

[35] L. M. Gan, J. Liu, L. P. Poon, C. H. Chew, Polymer 38 (1997) 5339–5345.

[36] T. H. Chieng, L. M. Gan, C. H. Chew, Polymer 37 (1996) 2801-2809.

[37] D. J. Johnson, F. Galiano, S. A. Deowan, J. Hoinkis, A. Figoli, N. Hilal, J. Membr. Sci. 484 (2015) 35-46

[38] W. Ming, F. N. Jones, S. Fu, Polymer Bulletin 40 (1998) 749–756.

[39] T. D. Li, L. M. Gan, C. H. Chew, W. K. Teo, L. H. Gan, Langmuir 12 (1996) 5863-5868.

[40] D. J. Johnson, N. Hilal, Desalination 356 (2015) 149-164.

[41] R. W. Bowen, T. A. Doneva, J. Coilloid Interface Sci. 229 (2000) 544-549.

[42] E. Guillen-Burrieza, R. Thomas, B. Mansoor, D. Johnson, N. Hilal, H. Arafat, J. Membr. Sci. 438 (2013) 126-139.

[43] V. Kochkodan, D. J. Johnson, N. Hilal, Adv. Colloid Interface Sci. 206 (2014) 116-140.

[44] M. Elimelech, X. Zhu , A. E. Childress, S. Hong, J. Membr. Sci. 127 (1997) 101-109.

[45] E. M. Vrijenhoek, S. Hong, M. Elimelech, J. Membr. Sci. 188 (2001) 115-128.

[46] D. Rana, T. Matsuura, R. M. Narbaitz, K. C. Khulbe, J. Appl. Polym. Sci. 101 (2006) 2292-2303.

[47] R. N. Wenzel, J. Phys. Chem. 53 (1949) 1466–1467.

[48] J. L. Liu, Y.Mei, R. Xia, Langmuir 27 (2011) 196-200.

[49] J. L. Liu, R. Xia, X. H. Zhou, Science China Physics, Mechanics & Astronomy 55 (2012) 1-9.

[50] T. D. Li, L. M. Gan, C. H. Chew, W. K. Teo, L. H. Gan, J. Membr. Sci. 133 (1997) 177–187.

[51] G. M. Litton, T. M. Olson, J. Colloid Interf. Sci., 165 (1994) 522-525.

[52] M. Elimelech, J. Gregory, X. Jia, R. A. Williams, in: Particle deposition and aggregation: measurement, modelling, and simulation, Butterworth-Heinemann, Oxford, 1995.

[53] Y. Sui, Z. Wang, X. Gao, C. Gao, J. Membr. Sci. 413–414 (2012) 38–47.

[54] X. Chen, Y. He, C. Shi, W. Fu, S. Bi, Z. Wang, L. Chen, J. Membr. Sci. 469 (2014) 447–457.

[55] H. Jang, D. H. Song, I. C. Kim, Y. N. Kwon, J. Appl. Polym. Sci. 132 (2015) DOI: 10.1002/APP.41712.

[56] A. Sweity, W. Ying, S. Belfer, G. Oron, M. Herzberg, J. Membr. Sci. 378 (2011) 186–193.

[57] Y. Zhang, M. Zhang, F. Wang, H. Hong, A. Wang, J. Wang, X. Weng, H. Lin, Bioresour. Technol. 152 (2014) 7–14.

[58] S. Sanguanpak, C. Chiemchaisri, W. Chiemchaisri, K. Yamamoto, Int. Biodeterior. Biodegrad. 102 (2015) 64–72.

[59] F. Meng, S.-R. Chae, A. Drews, M. Kraume, H.-S. Shin, F. Yang, Water Res. 43 (2009) 1489–1512.

[60] O. T. Iorhemen, R. A. Hamza, J. H. Tay, Membranes 6 (2016) 1-29.

[61] M. Sarayu, S. Shalini, D. Jyoti, M. Datta, Bioresource Technol. 99 (2008) 562–569.

[62] M. Elimelech, Z. Xiaohua, A. E. Childress, H. Seungkwan, J. Membr. Sci. 127 (1997) 101–109.

[63] E. Reid, X. Liu, S. J. Judd, J. Membr. Sci. 283 (2006) 164–171.

[64] K. N. Yogalakshmi, K. Joseph, Bioresource Technol. 101 (2010) 7054–7061.

[65] M. A. H. Johir, S. Vigneswaran, J. Kandasamy, R. Benaim, A. Grasmick, Desalination 322 (2013) 13–20.

[66] J. M. Hong, W. B. Li, B. Lin, M. C. Zhan, C. D. Liu, B. Y. Chen, Desalination 316 (2013) 23-30.

[67] R. Mancuso, R. Amuso, B. Armentano, G, Grasso, V. Rago, A. R. Cappello, F. Galiano, A. Figoli, G. De Luca, J. Hoinkis, B. Gabriele, ChemPlusChem 82 (2017) 1-11.

GRAPHICAL ABSTRACT